

Long-Range Interferometric Displacement Sensing With Tapered Optical Fiber Tips

Carlos J. Moreno-Hernández, David Monzón-Hernández, *Member, IEEE*, Alejandro Martínez-Ríos, David Moreno-Hernández, and Joel Villatoro

Abstract—A Fabry-Perot interferometer built with a properly selected tapered optical fiber tip and a flat reflecting target is proposed for long range displacement sensing. By scaling down the diameter of the core and cladding of the optical fiber that forms the interferometer, the divergence of the output beam is reduced. The tapered fiber tip also couples the reflected light from the target more efficiently. As a result, well-defined interference patterns are observed even for long cavities which allows to sense displacements as long as 80 mm. The fabrication of the fiber tips is simple and reproducible and the interrogation of the interference patterns is fast as a conventional fiber Bragg grating interrogator can be used. The possibility of multiaxis displacement sensing is discussed.

Index Terms—Fabry-Perot fiber interferometer, enhanced visibility, tapered optical fiber tip, displacement sensor, distance metrology.

I. INTRODUCTION

DISPLACEMENT (distance) sensing is important in a number of industrial and scientific applications, including for example, precision alignment, position monitoring, atomic-resolution microscopy, vibrations analysis, robotics, etc. Several optical techniques have proposed for displacement sensing [1], however, those based on optical fibers have several distinctive advantages as e.g. fast and contactless measurements, high resolution, compact size, immunity to electromagnetic interference [2]–[15]. So far a number of fiber optic displacement sensors have been reported in the literature, the most popular ones are based on intensity modulation and interferometry [6]–[15]. The former typically use optical fibers with high numerical aperture or fiber bundles to collect as much reflected light as possible from a flat reflecting target [6]–[8]. In interferometric displacement sensors, changes in distance alter the optical path difference between two interfering beams

Manuscript received September 22, 2014; revised November 7, 2014; accepted November 21, 2014. Date of publication November 26, 2014; date of current version January 21, 2015. The work of C. J. Moreno-Hernández was supported by the Mexican National Council for Science and Technology with the Ph.D. Fellowships through the Estancias de Consolidación Project under Grant 217697.

C. J. Moreno-Hernández, D. Monzón-Hernández, A. Martínez-Ríos, and D. Moreno-Hernández are with the Centro de Investigaciones en Óptica, A.C., León 37150, Mexico (e-mail: jcarlosbrown@gmail.com; dmonzon@cio.mx; amr6@cio.mx; dmh@cio.mx).

J. Villatoro is with the Department of Communications Engineering, Escuela Técnica Superior de Ingeniería de Bilbao, University of the Basque Country, Bilbao E-48013, Spain, and also with IKERBASQUE—Basque Foundation for Science, Bilbao E-48011, Spain (e-mail: agustínjoel.villatoro@ehu.es).

Color versions of one or more of the figures in this letter are available online at <http://ieeexplore.ieee.org>.

Digital Object Identifier 10.1109/LPT.2014.2375651

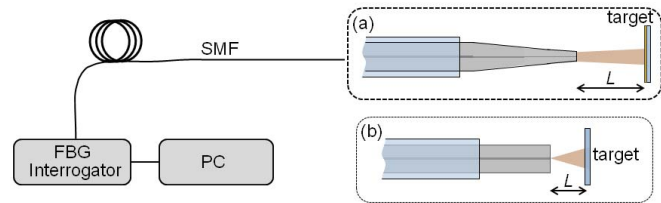


Fig. 1. Schematic diagram of the displacement measurement set up that includes standard single mode fiber; a fiber Bragg grating (FBG) interrogator controlled with a personal computer (PC), and Fabry-Perot interferometry cavity. The latter is formed between a tapered optical fiber tip and target (a) as an alternative to cleaved fiber end and target (b). L is the distance between the fiber tip and target.

which results in a detectable shift of the interference pattern. Intensity modulated sensors offer low resolution and large measuring range. However, their accuracy is affected by random fluctuations of the optical source or uncontrollable attenuations in the optical fiber junctions. Interferometric displacement sensors offer ultra-high precision but the measuring range is typically limited to few millimeters [10]–[13]. In addition, they tend to be more complex.

Fabry-Perot interferometry offers one of the simplest approaches to sense displacement [10]–[15], see Fig. 1. The Fabry-Perot interferometer (FPI) can be built with just a cleaved optical fiber separated a distance L from a flat reflecting target [10], [11]. In a FPI, the period, amplitude and/or wavelength position of the peaks and notches of the interference pattern depend on L . As period, phase, or shift of the interference pattern can be measured with high accuracy, sub-nanometer displacements can be sensed with an optical fiber FPI [11], [12]. The main limitation of most FPIs reported until now is the short measuring range that is typically a few millimeters due to the high divergence of the output beam of the optical fiber, see Fig. 1. To overcome this limitation Thurner *et al.* proposed the use of collimating or focusing lenses at the end of the optical fiber and corner cube mirrors attached to the moving target [14]. Another possibility is to splice graded-index multimode fiber to a single-mode fiber [15]. The disadvantages of the aforementioned approaches are the critical alignment and bonding of the opto-mechanical pieces and the bulkiness of the final device.

In this letter, we demonstrate that a FPI built with a suitable tapered optical fiber tip and a reflecting target it is possible to measure displacements of up to 80 mm without compromising resolution, robustness, or simplicity. Tapered fiber tips not only diminish the divergence of the output fiber beam but they

are also more efficient to collect the reflected light from the target. In addition, they are mechanically and thermally stable. The interference patterns can be monitored, e.g., with a fiber Bragg grating (FBG) interrogator which enables fast multi-axis displacement measurements.

II. DESIGN OF THE INTERFEROMETER AND RESULTS

Our FPI is built with a tapered optical fiber tip separated a distance L from a flat reflecting target, see Fig. 1. In our FPI the key element is the tapered optical fiber tip. To fabricate low-loss fiber tapers with any profile we used a computer-controlled glass processing workstation (Vytran GPX-3000). The waist diameter of the fabricated tapers was between 85 to 55 μm . Immediately after the tapering process the optical fibers were cleaved in the thinnest section with a high-precision optical fiber cleaver (Vytran LDC-200). The fabrication of the fiber tips is simple, inexpensive, highly reproducible, and takes only a few minutes. To ensure that mode coupling in the tapers did not occur we measured the reflection spectra of the tapered fiber tips. Only those samples that did not exhibit any modulation and those with negligible losses were used in the experiments.

The reason we used a tapered fiber tip is to reduce, in a simple but effective manner, the divergence of the output beam of the optical fiber. In an adiabatically tapered optical fiber the effective refractive index transition varies along the longitudinal direction, causing efficient mode coupling of the fundamental core mode to a local fundamental mode of the taper waist [16]–[21]. During the tapering process, both the fiber core and cladding diameter decrease by the same proportion, allowing the ratio of cladding to core diameter, R , being fixed. The effective index of the fundamental mode, n_{eff} , also decreases monotonically with taper diameter and will coincide with the cladding index at a specific taper diameter, known as the core-mode cutoff diameter. At this diameter the fundamental mode is no longer confined to the core and propagates unattenuated in the cladding [18], [19].

As the core diameter decreases the V-parameter of the fiber linearly decreases [16] and consequently, the mode field diameter increases until the core-mode cutoff diameter is reached. At this point $V = V_t = \{2/\ln(R)\}^{(1/2)}$ [19] the mode field diameter reaches its maximum for the core guided fundamental mode [16], [18], [19]. For a standard single-mode fiber, cutoff diameter is close to 53 μm and $V_t = 0.8568$. Beyond that diameter the fundamental mode is guided by the cladding/air waveguide and the spot size starts to decrease [18]. At this diameter, the output beam from a cleaved optical fiber tapered tip diverges much less than that of an un-tapered tip. Moreover, this optical fiber tip couples more efficiently the reflected light from the target than an un-tapered tip since the collecting area includes the cladding region of the fiber taper tip.

In order to confirm the assertions found in [16], [18], and [19] we performed a simulation to obtain the corresponding effective index of the local mode of a tapered waveguide versus tapering diameter. In the fiber taper diameters considered here light is weakly guided by the core.

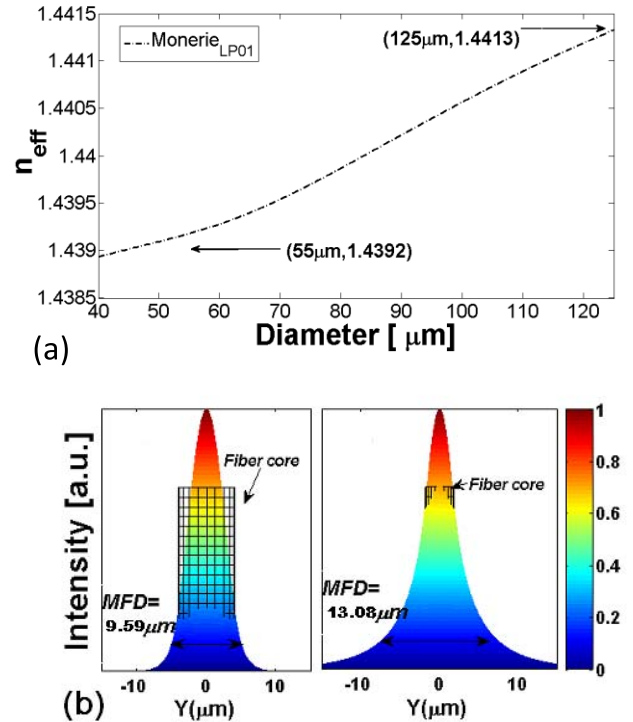


Fig. 2. (a) Computational solution for n_{eff} in monomode tapered fiber vs. tapered fiber diameter. (b) Representation of fundamental mode distribution in untapered (left) and tapered fiber (right).

The scalar approximation solution proposed in [22], which assumes that core guided mode is not affected by the cladding surrounding boundary, was used to calculate the effective index (n_{eff}) of the fundamental local mode despite its proximity to the n_{cladding} value. The fundamental local mode n_{eff} trend as a function of the fiber taper diameter is shown in Fig.2a).

With the corresponding n_{eff} and tapered fiber parameters we obtained the field components (E, H) and then the intensity pattern for the fundamental mode as stated in [23] for the step-index profile fiber. In Fig.2b) we observe how the light is distributed inside the waveguide comparing the size of the corresponding fiber core and the mode field diameter in each case. The fundamental mode increases 36.4% and fiber light coupling increases in the same amount in respect to standard single mode fiber which explains the enhanced visibility shown by the measures achieved.

When the beam leaves the fiber the optical phenomena is described by the following transfer function in a mathematical form,

$$I = I_R + I_S + 2\sqrt{(I_R I_S)} \cos\left(\frac{4\pi L}{\lambda} + \varphi_0\right) \quad (1)$$

In Eq. (1) I is the intensity of the resulting interference between two beams whose intensities can be denoted as I_R (the intensity of the beam internally reflected from the cleaved fiber tip) and I_S (the intensity of the beam that is coupled back into the tapered fiber tip after being reflected from the moving target). L is the distance between the fiber tip and the target, λ is the wavelength of the light, and φ_0 is the initial phase difference. It is clear from Eq. (1) that if light from a

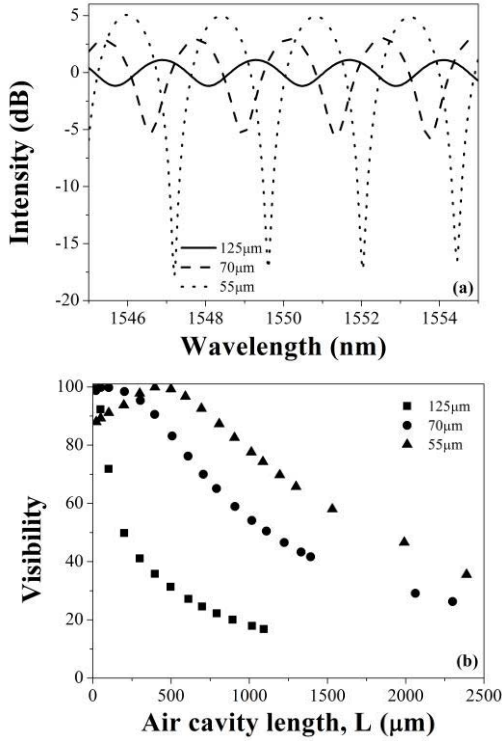


Fig. 3. (a) Experimental reflection spectra observed when the diameter of the optical fiber tip was 125 (untapered fiber), 70 and 55 μm . In all cases L was 500 μm . (b) Visibility of the interference patterns observed at different values of L for different tapered fiber tip diameters.

broadband source is fed to the tip -by means of a suitable fiber optic circulator or coupler- and the reflected light is analyzed with a spectrometer, then, the reflection spectrum will exhibit a modulation. The period, amplitude and wavelength position of the peaks/notches of the interference pattern are determined by the distance between the fiber tip and the target.

A detailed experimental investigation was carried out to find the optimal diameter of the fiber tip for displacement sensing. To do so, light from a super-luminescent LED (SLED, EXALOS), centered at 1550 nm and a bandwidth of 150 nm, was guided to the tapered fiber tips by means of a 3-dB (2X1) coupler. As a target we used a cleaved optical fiber. The reflected light was fed to an optical spectrum analyzer (AQ6370B, Yokogawa). Fig. 3a) shows the reflection spectra of our FPIs when the fiber tip had diameters of 70 or 55 μm and $L = 500 \mu\text{m}$. For comparison we show the case when the fiber was not tapered (tip diameter of 125 μm). The reflection spectra were also measured for different values of L and for different diameters of the fiber tips. Fig. 3b) shows the visibility of the interference patterns. The visibility was calculated with the following expression:

$$\text{Visibility} = \frac{(I_{\text{Max}} - I_{\text{Min}})}{(I_{\text{Max}} + I_{\text{Min}})}, \quad (2)$$

where I_{Max} and I_{Min} are, respectively, the intensity of the maximum and minimum values of the linear spectrum modulation around the central wavelength of the light source used, which in our case was 1550 nm. It can be noted from Fig. 3b) that the visibility drastically drops when the optical fiber is not tapered. However, when the fiber tips had diameters

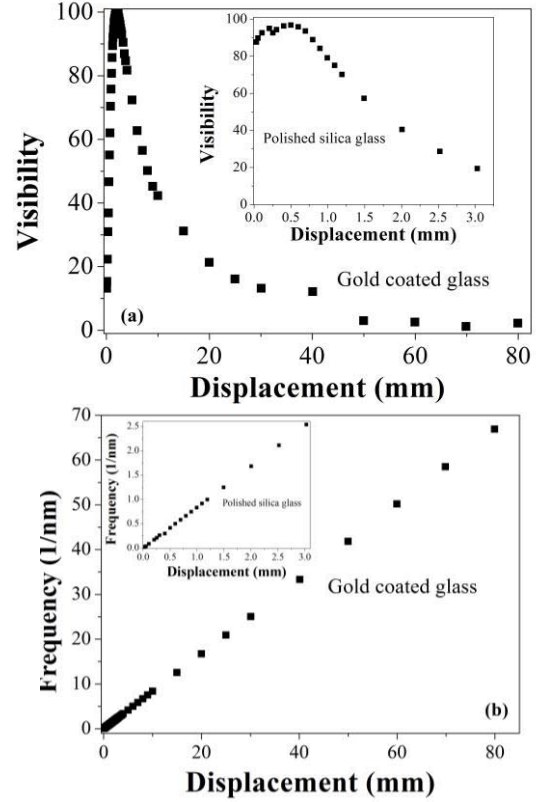


Fig. 4. (a) Visibility of the interference pattern as a function of L (distance) for the case when the target had low (inset) and high reflectivity. (b) Frequency of the FFT as a function of displacement for a low (inset) and high-reflectivity target. The fiber tip diameter was 55 μm in all cases.

less than 80 μm , visibility $>20\%$ even when L was 2500 μm . In our characterization we consistently observed that a fiber tip with diameter of 55 μm gave well-defined interference patterns even for long cavities. The reason for this response is that at this diameter the mode field radius reaches a maximum since it is very close to the core-mode cutoff diameter.

To measure distances we used a 55 μm -thick fiber tip for the reasons discussed above, and as a target we used a piece of flat fused silica glass (reflectance of 4.2%) and a gold-coated Pyrex glass slice (reflectance of 90% at 1550 nm). The fiber tip and the target were mounted on precision translation stages. The optical fiber with the tip in one extreme was fusion spliced to a FC patchcord and was connected to an FBG interrogator (Micron Optics, SM-125). We used an FBG interrogator because it has multi-channel capability and good sampling speed (up to several Hz).

To determine the cavity length (L in our case) we calculated the fast Fourier transform (FFT) of the interference patterns. It is known that the FFT of a sinusoidal pattern with period P exhibits a single peak at a spatial frequency $v = 1/P$. The FFT gives the period, hence L , with high precision even when the interference pattern exhibits poor visibility. To calculate in real time the FFT of the reflection spectra from the FBG interrogator we developed an *ad hoc* LabVIEW program.

In Fig. 4 we show the visibility of the interference patterns observed at different values of L and the peak frequency of the FFT as a function of the displacement of the target when

it had high and low reflectivity. When the reflectivity of the target was low, the measuring range was around $4000 \mu\text{m}$. However, for a high-reflectivity target the measuring range was extended up to $80000 \mu\text{m}$ demonstrating the advantages of using a tapered fiber tip to build a FPI.

To further study the capability of our displacement sensor we monitored displacements in steps of $5 \mu\text{m}$ when L was short. We found that displacements of around $1 \mu\text{m}$ could be resolved when L was $500 \mu\text{m}$. A simple manner to resolve nanometric displacements is to monitor the phase shift (instead of the period) of the interference pattern. The FFT gives, with high precision, the phase of the interference pattern [11]. Consequently, by monitoring the period and phase of the interference pattern of the FPI presented here it is possible to monitor large displacements with high resolution.

III. CONCLUSION

A simple optical fiber displacement sensor was proposed and demonstrated. The sensor is based on Fabry-Perot interferometry with the peculiarity that the interferometer is built with an adequate tapered optical fiber tip and a flat reflecting target. The tapered fiber tip plays a dual role in our FPI. On one hand, it reduces the divergence of the output beam of the optical fiber. On the other hand, it couples more efficiently the light reflected from the moving target. These two factors allowed us to measure distances from a few micrometers to up to 80 mm . The measuring range here demonstrated, along with the high resolution (typically of interferometric techniques), are large and high enough for many scientific and industrial applications.

The use of an FBG interrogator to monitor the interference patterns makes possible to measure multi-axis displacements with high speed. Therefore, we believe that the concepts and ideas here proposed are appealing, particularly for real-world applications that require ultra compact and precise displacement or distance sensors.

ACKNOWLEDGEMENTS

The authors would like to thank Karapetyan, K., Alt, W. and Meschede, D. for sharing their Optical fibre toolbox for Matlab code used with some modifications for our simulations.

REFERENCES

- [1] G. Berkovic and E. Shafir, "Optical methods for distance and displacement measurements," *Adv. Opt. Photon.*, vol. 4, no. 4, pp. 441–471, Dec. 2012.
- [2] Y. Zhao, P. S. Li, C. S. Wang, and Z. B. Pu, "A novel fiber-optic sensor used for small internal curved surface measurement," *Sens. Actuators A, Phys.*, vol. 86, no. 3, pp. 211–215, Nov. 2000.
- [3] T. Qi *et al.*, "Cladding-mode backward-recoupling-based displacement sensor incorporating fiber Up taper and Bragg grating," *IEEE Photon. J.*, vol. 5, no. 4, Aug. 2013, Art. ID 7100608.
- [4] C. Baker and X. Bao, "Displacement sensor based on Kerr induced phase-modulation of orthogonally polarized sinusoidal optical signals," *Opt. Exp.*, vol. 22, no. 8, pp. 9095–9100, Apr. 2014.
- [5] C. Ji, C.-L. Zhao, J. Kang, X. Dong, and S. Jin, "Multiplex and simultaneous measurement of displacement and temperature using tapered fiber and fiber Bragg grating," *Rev. Sci. Instrum.*, vol. 83, no. 5, p. 053109, 2012.
- [6] R. O. Cook and C. W. Hamm, "Fiber optic lever displacement transducer," *Appl. Opt.*, vol. 18, no. 19, pp. 3230–3241, Oct. 1979.
- [7] L. Perret, L. Chassagne, S. Topçu, P. Ruaux, B. Cagneau, and Y. Alayli, "Fiber optics sensor for sub-nanometric displacement and wide bandwidth systems," *Sens. Actuators A, Phys.*, vol. 165, no. 2, pp. 189–193, Feb. 2011.
- [8] H. Z. Yang, X. G. Qiao, D. Luo, K. S. Lim, W. Chong, and S. W. Harun, "A review of recent developed and applications of plastic fiber optic displacement sensors," *Measurement*, vol. 48, pp. 333–345, Feb. 2014.
- [9] M. Bravo, J. M. Baptista, J. L. Santos, and M. Lopez-Amo, and O. Frazao, "Micro-displacement sensor combined with a fiber ring interrogated by an optical time-domain reflectometer," *IEEE Sensors J.*, vol. 14, no. 3, pp. 793–796, Mar. 2014.
- [10] Y.-J. Rao, "Recent progress in fiber-optic extrinsic Fabry-Perot interferometric sensors," *Opt. Fiber Technol.*, vol. 12, no. 3, pp. 227–237, Jul. 2006.
- [11] T. Wang, S. Zheng, and Z. Yang, "A high precision displacement sensor using a low-finesse fiber-optic Fabry-Pérot interferometer," *Sens. Actuators A, Phys.*, vol. 69, no. 2, pp. 134–138, Aug. 1998.
- [12] N. O. Azak, M. Y. Shagam, D. M. Karabacak, K. L. Ekinci, D. H. Kim, and D. Y. Jang, "Nanomechanical displacement detection using fiber-optic interferometry," *Appl. Phys. Lett.*, vol. 91, no. 9, p. 093112, 2007.
- [13] A. A. Jasim, A. Z. Zulkifli, M. Z. Muhammad, S. W. Harun, and H. Ahmad, "A new compact micro-ball lens structure at the cleaved tip of microfiber coupler for displacement sensing," *Sens. Actuators A, Phys.*, vol. 189, pp. 177–181, Jan. 2013.
- [14] K. T. Thurner, P. F. Braun, and K. Karrai, "Fabry-Pérot interferometry for long range displacement sensing," *Rev. Scient. Instr.*, vol. 84, no. 9, pp. 095005-1–095005-10, Sep. 2013.
- [15] Y. Zhang *et al.*, "Fringe visibility enhanced extrinsic Fabry-Perot interferometer using a graded index fiber collimator," *IEEE Photon. J.*, vol. 2, no. 3, pp. 469–481, Jun. 2010.
- [16] R. Keil, E. Klement, K. Mathyssel, and J. Wittmann, "Experimental investigation of the beam spot size radius in single-mode fibre tapers," *Electron. Lett.*, vol. 20, no. 15, pp. 621–622, Jul. 1984.
- [17] K. P. Jedrzejewski, F. Martinez, J. D. Minelly, C. D. Hussey, and F. P. Payne, "Tapered-beam expander for single-mode optical-fibre gap devices," *Electron. Lett.*, vol. 22, no. 2, pp. 105–106, Jan. 1986.
- [18] J. D. Love, "Spot size, adiabaticity, and diffraction in tapered fibers," *Electron. Lett.*, vol. 23, no. 19, pp. 993–994, Sep. 1987.
- [19] J. D. Love, W. M. Henry, W. J. Steward, R. J. Black, S. Lacroix, and F. Gonthier, "Tapered single-mode fibres and devices. I. Adiabaticity criteria," *IEE Proc. J. Optoelectron.*, vol. 138, no. 5, pp. 343–354, Oct. 1991.
- [20] J. Bures, *Guided Optics: Optical Fibers and All-Fiber Components*. Hoboken, NJ, USA: Wiley, 2009.
- [21] B. Hubner *et al.*, "Laser diodes with integrated spot-size transformer as low-cost optical transmitter elements for telecommunications," *IEEE J. Sel. Topics Quantum Electron.*, vol. 3, no. 6, pp. 1372–1383, Dec. 1998.
- [22] M. Monerie, "Propagation in doubly clad single-mode fibers," *IEEE J. Quantum Electron.*, vol. 18, no. 4, pp. 535–542, Apr. 1982.
- [23] W. Snyder and J. D. Love, *Optical Waveguide Theory*. London, U.K.: Chapman & Hall, 1983.